

Self-Assembly of Chiral DNA Nanotubes

James C. Mitchell, J. Robin Harris,[†] Jonathan Malo, Jonathan Bath, and Andrew J. Turberfield*

Clarendon Laboratory, Department of Physics, University of Oxford, Parks Road, Oxford OX1 3PU, UK

Received October 7, 2004; E-mail: a.turberfield@physics.ox.ac.uk

A system of DNA “tiles” that is designed to assemble to form two-dimensional arrays is observed to form narrow ribbons several micrometers in length. Their uniform width and straight edges lead us to propose that they are arrays that have curled and closed on themselves to form tubes. This proposal is confirmed by the observation of tubes with helical order.

The specificity of base pairing makes DNA particularly suitable for nanofabrication.¹ Periodic arrays up to a few micrometers in size can be assembled by a hierarchical process in which smaller self-assembled tiles are held together by weak interactions between short “sticky ends”.² For this study we have used a system of two DAE-O double crossover tiles³ (Figure 1A): the four single-stranded sticky ends on each tile are arranged such that α and β tiles tessellate as shown in Figure 1B.

PAGE-purified DNA strands were mixed at a concentration of 1.6 μ M in a buffer containing 20 mM Tris-acetate pH 8.3 supplemented with 60 mM MgCl₂ (high salt buffer) or 12.5 mM MgCl₂ (low salt buffer). The strands were cooled from 96 °C to room temperature over 96 h using a linear temperature gradient. Figure 2 shows transmission electron micrographs of specimens spread across carbon support films and negatively stained. The central strand of the β tile (Figure 1A) was biotinylated at its 5' end and labeled by incubation with a 173.6 kDa streptavidin–antibody fusion protein (single chain variable fragment: scFvSA)⁴ (Figure 2, A–H, J) or a streptavidin–horseradish peroxidase conjugate (Sigma) (Figure 2I).

In high salt buffer we observe sheets and ribbons of DNA with periodic banding corresponding to the rows of streptavidin-decorated β tiles (Figure 2, A and B). In low salt buffer (Figure 2, C–F) we observe ribbon structures many micrometers in length and 40–250 nm in width (Figure 2C). Higher magnification reveals transverse streptavidin bands with periodicity 31 ± 2 nm (Figure 2D), consistent with the designed two-dimensional array structure with the long axis of the tiles aligned along the ribbons. Similar structures, without banding, are observed when the streptavidin labels are omitted. The straight edges and uniform width of all these structures—ribbons and sheets—are striking. If finite arrays were to form with unsatisfied bonds along their edges (Figure 1B), then we would not expect to see straight edges perpendicular to the rows of α and β tiles. Such an edge, shown on the left-hand side of the array in Figure 1B, incorporates a greater density of favorable attachment sites, at which a single tile could be attached by two bonds, than does a ragged or angled edge such as that shown on the right. A natural explanation for the parallel edges of these structures is that arrays of tiles curl and close upon themselves to form tubes (Figure 1C). DNA tube formation has been suggested by other groups.^{5,6} There is a pronounced increase in electron transparency consistent with maxima in projected thickness at the edges of these structures as seen in negatively stained images of microtubules and membrane tubules.⁷

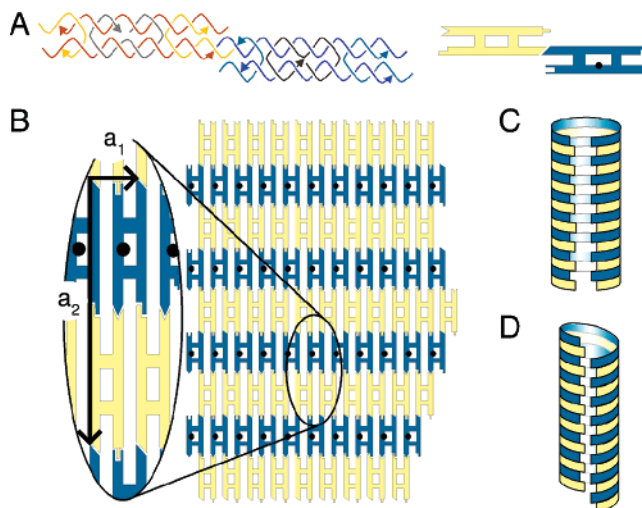


Figure 1. Self-assembly of DNA tiles into sheets and tubes. (A) Structure of the double crossover tiles: arrowheads mark the 3' end of each oligonucleotide. The 6 nt single-stranded sticky ends on the α tile are complementary to those on the β tile; complementary shapes on the schematic representations of the tiles indicate complementary sticky ends. The 5' biotin label on the β tile is represented by a black dot. (B) α and β tiles tessellate to form extended two-dimensional arrays. We propose that sheets can fold and close upon themselves to form tubes, producing either alternating rings (C) or nested helices (D) of α and β tiles.

Unambiguous evidence for the formation of tubes is provided by micrographs such as Figure 2E in which lines of streptavidin labels zigzag across a ribbon. In all such cases the line is continuous where it changes direction at the edge of the ribbon. These are helical tubes with a structure such as that illustrated in Figure 1D. The streptavidin zigzags do not exactly follow the sinusoidal path of a projected helix: in wider tubes we observe approximately straight segments with sharp bends at the ribbon's edges, suggesting that the tubes are flattened when deposited onto grids for electron microscopy. Occasionally we observe a tube which incorporates a defect so that it changes from nonhelical to helical part way along its length (Figure 2F).

As with carbon nanotubes,⁸ the structure of a DNA nanotube may be characterized by the indices (m, n) of wrapping vector $\mathbf{c} = m\mathbf{a}_1 + n\mathbf{a}_2$ where $\mathbf{a}_1, \mathbf{a}_2$ are basis vectors shown in Figure 1B and the tube is formed from a sheet by joining equivalent points separated by \mathbf{c} . We may count n exactly: it is equal to the number of nested helices of labeled β tiles. For nonhelical tubes $n = 0$ (Figure 2D); $n = 1$ where all labels lie on a single helix (Figure 2E). The short dimensions of the tiles are not resolved (the streptavidin labels are larger than the tile width); assuming $\mathbf{a}_1 = 4$ nm we estimate that for the tube in Figure 2E $m \approx 40$.

A variant β tile was designed to have a more flexible structure: a hairpin loop was added on the outside of the helix opposite the biotinylated nick (labeled by a black dot in Figure 1A). In high salt buffer this system forms larger sheets (Figure 2G)—these

[†] Institute of Zoology, University of Mainz, Mainz, Germany

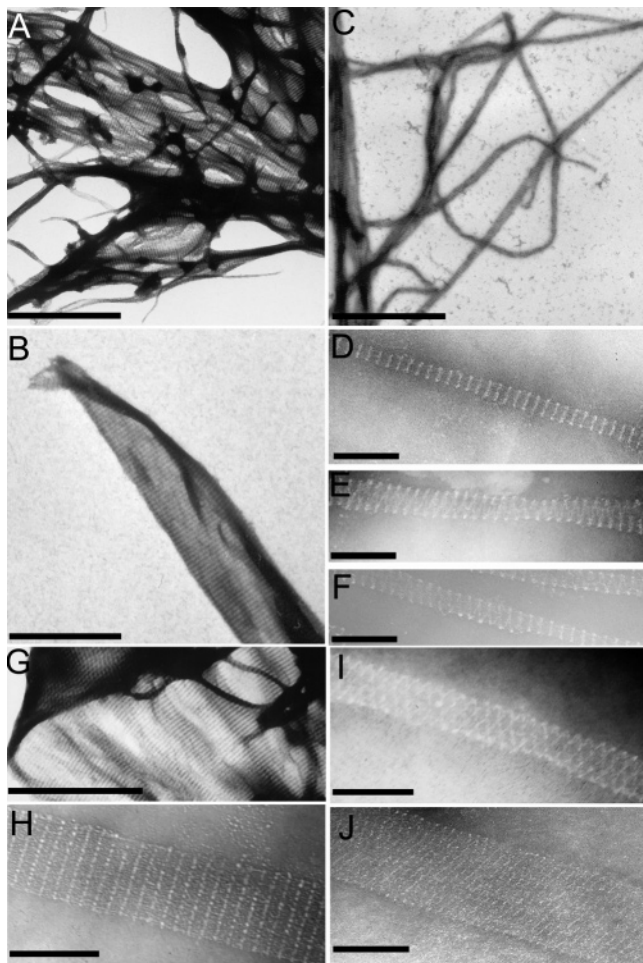


Figure 2. Transmission electron micrographs of negatively stained DNA nanotubes and arrays. Electron transparent dots correspond to protein labels bound to the centers of β tiles. The scale bar in A, B, C, and G is 1 μm in length; in D, E, F, H, I, and J the scale bar is 200 nm in length.

frequently have parallel edges at which there is increased contrast and which run perpendicular to the rows of β tiles, suggesting that these large structures, too, are tubes. In low salt buffer the modified tile produces both $(m,0)$ tubes (Figure 2H) and (m,n) tubes with $n > 1$; Figure 2J shows a $(\sim 120,6)$ tube in which the streptavidin labels lie on 6 nested helices. The measured spacing between streptavidin bands falls as n increases, most markedly to ~ 20 nm in Figure 2J. We do not resolve the corresponding structural changes, which may reflect either preferred directions of folding at the edges of a flattened tube or a preferred alignment of the tube axis with a particular lattice vector to minimize the strain energy of the curved surface. Distortion of the unit cell may be facilitated by disruption of base stacking at nicks (in the central strands and where sticky ends overlap) and where the hairpin protrudes.

It is likely that tube diameters are determined by nonequilibrium processes: once a tube has closed, an activation barrier prevents further lateral growth. Tube formation reduces the free energy of a tile array by satisfying all intertile bonds except those at the ends of the tube. Intrinsic curvature of the array would facilitate tube formation, but the half-integral number of helical turns along the arms joining crossover points on adjacent tiles means that the intrinsic curvatures of α and β tiles are opposed. We deduce from the observation of extended two-dimensional structures in our own high-salt samples and in other studies of similar DAE-O arrays^{2,9} that intrinsic curvature is relatively small. The strain energy penalty

for tube formation is then $\pi D_{\perp}/r$ per unit length, where r is the tube radius and D_{\perp} the flexural rigidity (bending modulus) of a DAE-O array corresponding to a curvature axis perpendicular to the long axis of the tiles. We estimate an upper limit to D_{\perp} by considering the stability of our narrowest tubes ($r \approx 20$ nm). The bond spacing along a potential rupture line running along the tube is $a_2/2$; the bond energy ΔG_{bond} is ~ 10 kcal/mol at room temperature;¹⁰ by requiring that $\pi D_{\perp}/r + 2\Delta G_{\text{bond}}/a_2 < 0$ we obtain $D_{\perp} < 3 \times 10^{-20}$ J. This is consistent with the prediction of a model in which the array bends by twisting the arms joining tiles: $D_{\perp} \approx 6 \times 10^{-21}$ J (see Supporting Information). For comparison we estimate the flexural rigidity for curvature *along* the tile axis to be $D_{\parallel} \approx 10^{-19}$ J.

Wide carbon nanotubes collapse under van der Waals forces;¹¹ the flattening of our larger tubes is consistent with an attractive interaction between sheets of tiles¹² that, above a critical radius, can overcome elastic forces to cause tube collapse. Wide, folded structures, such as those we observe in high salt buffer, might be produced if collapse (folding) were to precede tube closure.

Helical DNA nanotubes form a new class of nanostructure. DNA is intrinsically chiral (each nucleotide incorporates D-deoxyribose); our helical tubes have an additional mesoscopic structural chirality, analogous to that of chiral carbon nanotubes, that results from the pattern of connections between tiles. They could be used to construct helical tracks down which free-running DNA motors could ferry cargos.¹³ Protein structure determination by cryo-electron microscopy of helical structures has been achieved for microtubules, bacterial flagellae,¹⁴ and membrane tubules containing the acetylcholine receptor;¹⁵ our use of protein labels suggests that it may be possible to apply this technique to proteins bound to helical DNA nanotubes.¹⁶

Acknowledgment. TEM facilities were provided by Prof. L. N. Johnson, Laboratory of Molecular Biophysics, University of Oxford, and by Prof. A. Fischer, Institute of Zoology, University of Mainz. The streptavidin fusion protein (scFvSA) was kindly provided by the NeoRx company, Seattle, Washington, U.S.A.

Supporting Information Available: DNA sequences, sample preparation protocols and estimates of elastic properties of a DX array. This material is available free of charge via the Internet at <http://pubs.acs.org>.

References

- (1) Seeman, N. C. *Nature* **2003**, *421*, 427.
- (2) Winfree, E.; Liu, F.; Wenzler, L. A.; Seeman, N. C. *Nature* **1998**, *394*, 539.
- (3) Fu, T. J.; Seeman, N. C. *Biochemistry* **1993**, *32*, 3211.
- (4) Schultz, J.; Lin, Y.; Sanderson, J.; Zuo, Y.; Stone, D.; Mallet, R.; Wilbert, S.; Axworthy, D. *Cancer Res.* **2000**, *60*, 6663.
- (5) Yan, H.; Park, S. H.; Finkelstein, G.; Reif, J. H.; LaBean, T. H. *Science* **2003**, *301*, 1882.
- (6) Rothmund, P. W. K.; Ekani-Nkodo, E.; Papadakis, N.; Kumar, A.; Fyngenson, D. K.; Winfree, E. *J. Am. Chem. Soc.* **2004**, *126*, 16344.
- (7) Harris, J. R. *J. Ultrastruct. Res.* **1971**, *36*, 587; Harris, J. R.; Gerber, M.; Gebauer, W.; Wernicke, W.; Markl, J. *J. Microsc. Soc. Am.* **1996**, *2*, 43.
- (8) Dresselhaus, M. S.; Dresselhaus, G.; Eklund, P. C. *Science of Fullerenes and Carbon Nanotubes*; Academic Press: San Diego, 1996.
- (9) Liu, F.; Sha, R.; Seeman, N. C. *J. Am. Chem. Soc.* **1999**, *121*, 917.
- (10) Zuker, M. *Nucleic Acids Res.* **2003**, *31*, 3406.
- (11) Chopra, N. G.; Benedict, L. X.; Crespi, V. H.; Cohen, M. L.; Louie, S. G.; Zetti, A. *Nature* **1995**, *377*, 135.
- (12) Ruzina, I.; Bloomfield, V. A. *J. Phys. Chem.* **1996**, *100*, 9977.
- (13) Turberfield, A. J.; Mitchell, J. C.; Yurke, B.; Mills Jr., A. P.; Blakey, M. I.; Simmel, F. C. *Phys. Rev. Lett.* **2003**, *90*, 118102.
- (14) Nogales, E.; Wolf, S. G.; Downing, K. H. *Nature* **1998**, *391*, 199.
- (15) Yonekura, K.; Maki-Yonekura, S.; Namba, K. *Nature* **2003**, *424*, 643.
- (16) Malo, J.; Mitchell, J. C.; Vénien-Bryan, C.; Harris, J. R.; Johnson, L. N.; Sherratt, D. N.; Turberfield, A. J. Manuscript in preparation.

JA043890H